PROCEEDINGS OF SCIENCE

Calibration and monitoring of LHAASO-KM2A muon detectors with muon decay events

Xiong Zuo[*†]
IHEP, CAS,(Institute of High Energy Physics, Chinese Academy of Sciences), for the LHAASO Collaboration
E-mail: zuoxiong@ihep.ac.cn

Gang Xiao, Shaohui Feng, Xiurong Li, Cong Li, Ning Cheng, Lingyu Wang, Jinfan Chang, Wei Wang, Minghao Gu, Fei Li, Jia Liu, Hongkui Lv, Xiangdong Sheng, Huihai He
IHEP, CAS

Hongming Li, Guanghua Gong
Tsinghua University

The LHAASO Collaboration

The Large High Altitude Air Shower Observatory (LHAASO) will be constructed at 4400 m asl in Daocheng, Sichuan Province, with the aim of discovering sources of ultra-high energy cosmic rays and studying cosmic ray physics. The whole array includes 1171 muon detectors (MDs), constituting the largest muon detector array in the world. The special high altitude and wide-field environment requires simple and stable calibration as well as monitoring method of MDs. In this paper, the muon decay events will be selected for calibrating the charge and monitoring the water level of each MD. In the prototype muon detector, the simulation and experiment results reveal that the charge of the decay electron is approximately 0.147 times that of the vertical equivalent muon for a standard MD, and the Q_{VEM}/Q_e shows a linear correlation with the water level.

35th International Cosmic Ray Conference — ICRC2017
10–20 July, 2017
Bexco, Busan, Korea

[*] Speaker.
[†] The LHAASO Collaboration

PoS(ICRC2017)441

1. Introduction

The Large High Altitude Air Shower Observatory (LHAASO) will explore basic problems such as the origin of high-energy cosmic rays and relevant evolution of the universe, with the highest sensitivity to ultra-high energy gamma rays, the highest survey sensitivity to very high-energy gamma ray sources, and wide cosmic ray energy coverage [1][2][3]. Covering a total area of 1.2 km^2, LHAASO consists of a Kilometer-square Array (KM2A), a water Cherenkov Detector Array (WCDA) and a Wide-field Cherenkov Telescope Array (WFCTA).

As the main part of the LHAASO project, KM2A composes of electron detectors (EDs) and muon detectors (MDs), and more than 40000 m^2 area of muon detectors are uniformly distributed in a triangular grid with a spacing of 30 m throughout the whole array [4]. Such a large area of MDs would contribute to background-free observation of gamma rays, because gamma ray-induced showers contain scarce muons, whereas hadronic showers are abundant in muons [5]. The number of muons in hadronic showers is correlated with the nucleon number of primary hadrons and can be used to discriminate the compositions of primary hadrons [6][7], thus KM2A could help solve the problem in the cosmic rays spectrum at around the "knee" energy region ($10^{13} - 10^{18}$eV). Furthermore, information on muon content in hadronic showers helps in testing the hadronic interaction models [8][9][10][11].

The MD adopts water Cherenkov technique to detect secondary muons in showers of cosmic rays, and the basic design for MD units is described as follows [4]: pure water is sealed in a bag with a high reflective inner liner and the bag is then placed in a concrete tank with a diameter and height of 6.8 and 1.2 m, respectively. An 8 in. photomultiplier tube (PMT) is centered in the upper surface of the bag. A 2.5 m thick shielding soil covers the tank to eliminate the electromagnetic components in showers.

The calibration and monitoring of the MDs, which is necessary prior to data analysis, is not easy, especially for an MD array with a large area and situated in tough high-altitude environment. Thus, a convenient and steady online method is needed for MDs.

Most shower muons possess energies $> 1GeV$ and can penetrate the overburden soil. The charge of vertical equivalent muon (VEM) is closely related to the track length which is proportional to the water level. Moreover, the charge depends on several other factors, such as water absorption length, Tyvek reflectivity, PMT collection efficiency and the temperature effect of electronics and PMT. However, a low-energy muon is easily stopped in the tank water and decays, with a typical life time of approximately 2.2 μs, to two neutrinos and an electron which is called a Michel electron [12]. A Michel electron possesses an average energy of 37 MeV and a maximum energy of 53 MeV. Thus, the Michel electron mostly deposits all energy in the 1.2 m cylindrical tank, and the charge of the Michel electron is correlated with the factors above expect the water level. Thus, the charge ratio of VEM signals to the Michel electron signals (Q_{VEM}/Q_e) is only limited with the water level, which would be an effective and convenient solution for monitoring the sealing property of MD water bags, considering that the MDs are buried under 2.5 m thick soil. Furthermore, the charge peak of muon decay signal functions for the calibration of MD signal charge.

In this article, a unique approach is presented to achieve charge calibration and water level monitoring by selecting the muon decay events. The relation between Q_{VEM}/Q_e and water level according to the Geant4 simulation is shown and proven using the experiment data.

2. MC Simulation

The maximum track length of the Michel electron in MD is approximately 26.5 cm, with the electron deposition at approximately 2 MeV/cm in water. With a sufficiently deep water Cherenkov detector, the Michel electron deposits all of its enengy in the water, whereas the VEM passes through the water with deposition energy proportional to water depth D. Thus, Q_{VEM}/Q_e can be approximately described as follows:

$$\frac{Q_{VEM}}{Q_e} = \frac{N_{VEM} \cdot \eta_1 \cdot \eta_2 \cdots \eta_n}{N_e \cdot \eta_1 \cdot \eta_2 \cdots \eta_n} = \frac{D}{L_e}(D > 26.5cm) \tag{2.1}$$

where Q_{VEM} and Q_e are the charges of VEM signal and the Michel electron signal, respectively, N_{VEM} is the mean light yield of VEM in water, N_e is the mean light yield of Michel electron, L_e is the mean track length of the Michel electron, and $\eta_1, \eta_2, \cdots \eta_n$ are the collection efficiency or conversion efficiency determined by MD geometry, water absorption length, Tyvek reflectivity, PMT and electronics. Thus, the Q_{VEM}/Q_e is proportional to the water depth D when D is markedly higher than the maximum track lengh of the Michel electron (26.5 cm). A similar relationship between Q_{VEM}/Q_e and water level is achieved in the Auger experiment [13][14].

A vertical muon passing through the water tank possesses a track length equivalent to the water depth, and the Michel electron will leave an average track length of 18.5 cm. Hence, for a MD tank with a D value of 120 cm, the charge ratio will be approximately 6.5. According to preliminary calculations using the formula above, Q_{VEM}/Q_e would decrease by 0.83% as the water level decreases by 1 cm.

A dedicated Monte Carlo simulation program based on GEANT4 [15] is developed to simulate the detector responses to incident particles. Cherenkov photons are produced along the path of the injected muons and then track through water until the photons are absorbed or reach the active area of the PMT photocathode. For each event, a single muon is transferred into the Cherenkov water tank. The events are marked as stopping muons when the incident muons decay in the water, otherwise, the events are called pass-through muons. Moreover, The vertical muon events are simulated for this study.

Liner reflectivity and water absorption length is set to 97.5% and 150 m, respectively. Muons uniformly hit the whole tank, with zenith angle sampled according to $cos^6\theta$ and the azimuth angle sampled uniformly in the range of $0^\circ - 360^\circ$. The energy of each muon is obtained by sampling the energy spectrum of secondary muons in hadron-initiated showers. The water levels of the tank are set to several separated positions from 109cm to 120 cm.

The left panel of Fig.1 shows the charge distribution of Michel electrons and VEM in unit of number of photoelectrons (PEs). The water level was set to 120 cm, and the probability of a muon decay event was approximately 6.5%.

On each water level, the charge of muon decay signal and VEM signal can be achieved through simulation, and the relationship between the ratio of muon charge to the electron charge and the water level is shown on the right panel of Fig.1. The simulation results are in accordance with the estimates. Thus, a linear fit is applied to the simulation data, and the relationship between the water level D and Q_{VEM}/Q_e is described below:

$$\frac{Q_{VEM}}{Q_e} = (0.8307 \pm 0.0016)\% \cdot D(cm) \tag{2.2}$$

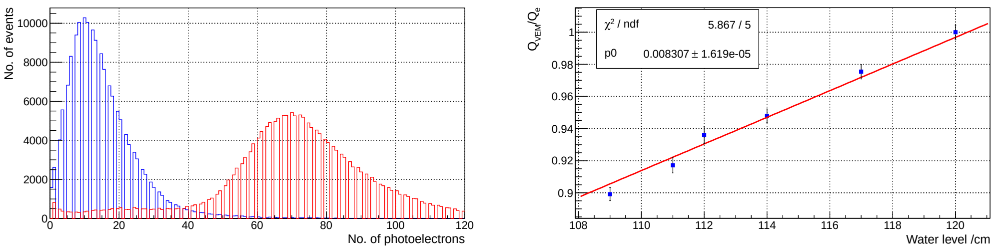

Figure 1: The left panel is the charge distribution of Michel electron (blue line) and VEM (red line) in simulation. The ratio of vertical muon charge to electron charge versus the water level by Geant4 simulation is drawn on the right panel, and a linear fit is applied. The values of vertical ordinate on right panel are normalized to that of 120 cm in water depth.

To test the effect of water absorption length and Tyvek reflectivity, we conduct the simulation with different values of these two parameters. The charge of VEM and the Michel electron markedly vary, however, the Q_{VEM}/Q_e is fairly consistent with that of the former parameter settings.

3. Experiment setup

Two MD prototypes have been built at the Yangbajing Cosmic Ray Observatory at the end of 2012 and in October 2014 [4]. Each tank is equipped with an 8 in. PMT, and both anode and dynode signals are transferred by coaxial cables to specific electronics which includes a 500 MHz 12-bit flash analog-to-digital converter (FADC) digitizing the signal and a field-programmable gate array (FPGA) processing the FADC data (Fig.2). When the anode signal amplitude exceeds a certain threshold, the trigger time, sum of charge and pedestal information will be packed as a hit and sent to the data acquisition system (DAQ) by a fiber based on the WR network [16]. Moreover, a 5 μs time window of digitized waveform of a hit is also sent to the DAQ every second by the MD front-end electronic (FEE).

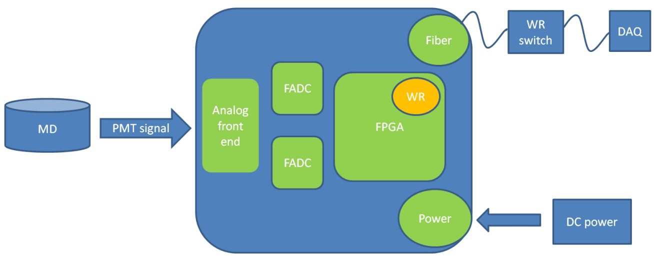

Figure 2: Schematic view of MD FEE and DAQ system.

One of the water bag in MD prototypes suffers a slight damage during the transport, and the water level measured by a position sensor decreases from 120 cm to 112 cm gradually within 8 months. This long-term leaking experiment is used to validate the relation between Q_{VEM}/Q_e and water depth achieved during simulation. Moreover, in the experiment, all information on MD hits are normally collected by electronics and sent to DAQ simultaneously for further analyses.

4. Data selection

Based on the waveform of each hit, two events are selected as the dedicated stopping muon event and muon decay event in the 5 μs time window. The trigger time is set to approximately 440 ns by FEE, therefore the charge of the first event (Q_1, in unit of number of PEs) is integrated from 400 ns to 1200 ns and the trigger time (T_1) is calculated by searching the maximum amplitude in the integral time window. Similarly, the trigger time of second event (T_2) is searched from 1400 ns to 4500 ns to avoid the influence of the first event given that the signal waveform is few hundred ns in width. Then, the charge of the latter (Q_2) is integrated within 800 ns. Finally, all four parameters are recorded for further analysis.

In the charge distribution, the Michel electron signals are completely drowned by background noise which is mainly dominated by the PMT after pulse, fluctuation of pedestal, PMT dark noise, and muons hitting in the corner of tank. To effectively select decay signals, several other special features must be found using the waveform information. Fig.3 shows the waveform of a muon decay event in the simulation. Similar to a single pass-through muon, Cherenkov lights produced by a Michel electron in the MD tank are reflected by the diffuse reflection material Tyvek and reach the PMT for many times. Hence, the waveform presents multiple separated clusters, and the time interval between the adjacent clusters is mainly due to the mean free path of photons between the two PMT hitting processes. In contrast, the time interval of the random background noise basically follows an exponential distribution.

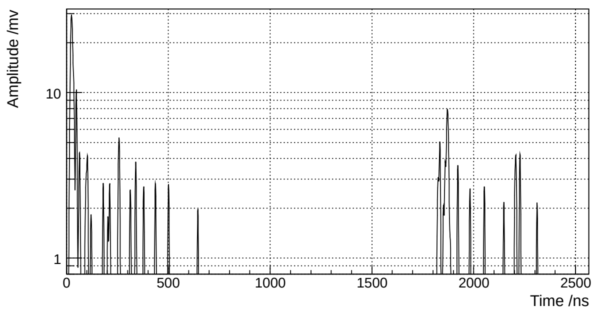

Figure 3: A waveform of muon decay event in simulation. The first part (<1000 ns) corresponds to a stopping muon signal and the second part is the waveform of the Michel electron signal.

Hence, a statistical variable T_c, called mean hitting time of PMT by photons, is constructed. In the data analysis, T_c is defined as below:

$$T_c = \frac{T_{sum}}{N_{cluster}-1}(N_{cluster} > 1) \tag{4.1}$$

where T_{sum} is the sum of the time intervals, that is, the waveform width, and $N_{cluster}$ is the number of PE clusters.

Each cluster is selected through searching the peak in the second integral time window, then, the time position of each peak is defined as the time of the corresponding cluster. The distribution of T_c is shown in Fig.4(the left panel). In the picture, an evident peak found at approximately 30 ns is mainly be contributed by the Michel electron and coincident background muons. The simulated T_c distribution of Michel electrons is drawn on the right panel. The relatively short track length of the Michel electron corresponds to the low light yield and would highly likely present a Poisson fluctuation in the number of PEs in each cluster, thereby resulting in a longer mean free path. Thus, the average time interval of the Michel electron exceeds that of a single pass-through muon to a certain extent.

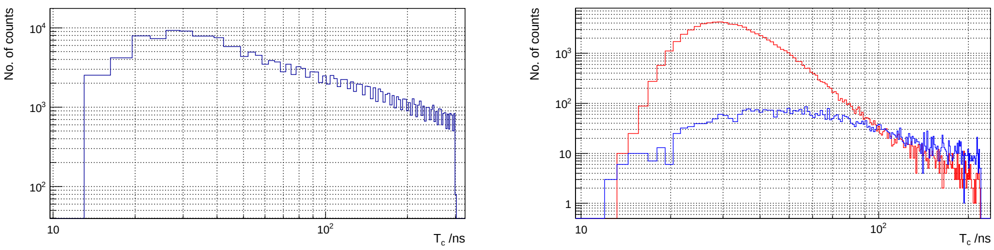

Figure 4: The left panel is the T_c distribution of the second event measured, and the evident peak is dominated by Michel electrons and background muons. The simulation result is shown on the right panel (red line for the single pass-through muon and blue line for the Michel electron).

The charge of the second events limited with a cut-off of T_c from 20 ns to 120 ns is plotted in Fig.5. Moreover, to decrease accidental coincidence, another cut-off of the charge of the first events (Q_1 <50 PEs) is applied considering that the charge peak of background muons is approximately 70 PEs and the charge of stopping muons presents a peak at 40 PEs according to the simulation result. In the figure of charge distribution, two apparent peaks can be found at approximately 10.5 and 70 PEs, which correspond to muon decay signal and single muon signal, respectively.

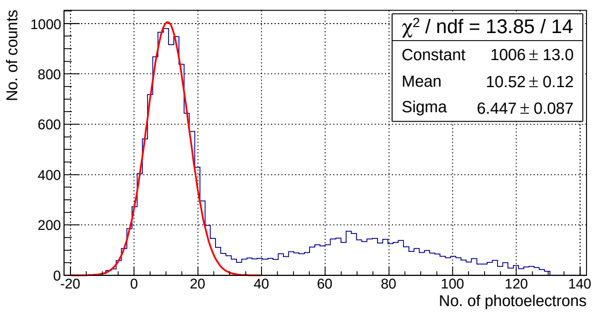

Figure 5: Charge of the events after a cut-off of T_c around the peak time 30 ns. The double peaks correspond to Michel electrons signal and background muons signal, respectively.

Thus, based on the former two cut-offs, another cut-off Q_2 <25 PEs can easily contribute to the search for relatively pure muon decay signals. The final event rate of muon decay events in experiment and simulation are approximately 0.208% and 0.199% that of all candidate events, respectively. Notably, the error of experiment results appears slightly large, and one crucial limitation is the statistics, which is dependent on the sample rate and time window of waveform collected by MD electronics.

In the leaking experiment, the water depth decreases from 120 cm to 112 cm gradually, and the charge of VEM signal and the Michel electron signal in different water level are shown in Fig.6. The charge of the Michel electron signal also decrease as the water level declines, because the water quality gradually deteriorates within 8 months, as validated by the measurement of decay time of the signal waveform.

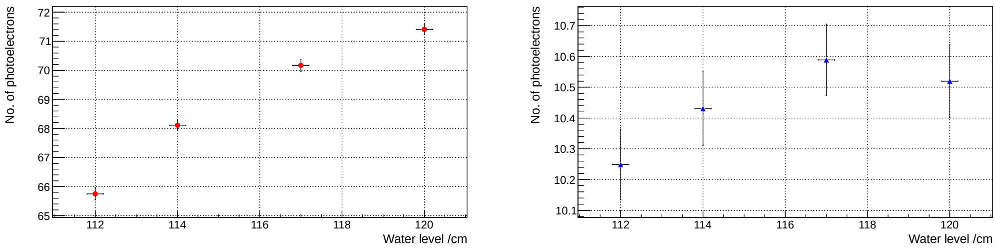

Figure 6: The left panel is the charge of VEM signal, and the charge of the Michel electron signal is shown on the left panel.

With the special experiment setup, water level as a function of the ratio of the VEM peak to the electron peak is drawn in Fig.7. The error bars correspond to an error of 0.2 cm in the water level determination. The longitudinal error bars are statistically significant with an error of approximately 0.011. The simulation result is shown in the panel. The water quality deteriorates, however, the simulation result is in relative agreement with the experimental data and an accuracy of approximately 1.3 cm of water level can be obtained using this method.

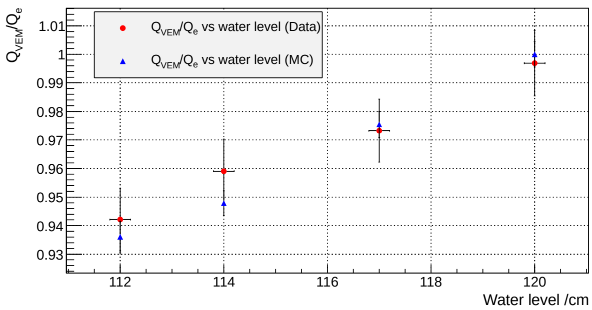

Figure 7: Q_{VEM}/Q_e versus water level. The blue and red dots correspond to the experiment and simulation result, respectively. The values of the vertical ordinate are normalized to that of the 120 cm water depth.

5. Summary and Conclusions

A new method using muon decay events has been established to calibrate and monitor MDs and studied using Geant4 simulation. The number of photoelectrons produced by the Michel electron is approximately 0.147 times that produced by the VEM for a standard MD at a 120 cm water depth. This method provides us with a complementary approach to calibrate the number of incident muons. Moreover, the Q_{VEM}/Q_e will help supply an online monitoring of the water level.

The simulation results have been commendably validated by prototype muon detectors in Tibet. In the experiment, muon decay events are effectively selected in the waveform data by constructing a statistical variable T_c and several relative cut-offs in the data analyses. A changing of water level experiment, similar to that of the Auger prototype [13], has been used to validate the simulation results, and an accuracy of 1.3 cm of water level can be attained from the muon decay method.

Acknowledgements

This work is supported by National Natural Science Foundation (NSFC) of China under contacts No.11635011 and 11605208.

References

[1] Z. Cao et al., LHAASO Collaboration, 31st ICRC, Lodz, (2009).

[2] Z. Cao., LHAASO Coll., CPC 34(2) (2010) 249-252.

[3] Z. Cao., LHAASO Coll., Frascati Physics Series Vol. 58(2014).

[4] X. Zuo, LHAASO Coll., Nuclear Instruments and Methods in Physics Research Section A 789 (2015) 143-149.

[5] Xinhua. Ma et al., LHAASO Coll., Astroparticle Physics 54 (2014) 86-92.

[6] J. W. Cronin, Nucl. Phys. B(Proc. Suppl), 2005, 138, 465.

[7] M. A. K. Glasmacher, Astropart. Phys. 1999, 12, 1.

[8] J. Zabierowski et al., KASCADE-Grande Coll., Proc. of 30th ICRC, Merida (2007), vol. 4: 111-114.

[9] W. D. Apel. et al., Astropart. Phys., 2011(34): 476-485.

[10] J.C. Arteaga et al., Proc. 33st ICRC, RIO DE JANEIRO, 2013, astroph.HE, arXiv:1308.3202v1.

[11] V. Souza et al., Proc. of the 32nd ICRC, Beijing (2011), ID 0953.

[12] L. Michel, Proc. Phys. Rep. A 63, 514 (1950).

[13] P. L. GHIA, FOR THE PIERRE AUGER COLLABORATIONčň30th ICRC, Mexico, 2007.

[14] M. Alarcon et al., Nuclear Instruments and Methods in Physics Research Section A 420 (1999) 39-47.

[15] J.Allison et al., IEEE Transactions on Nuclear Science NS-53(1)(2006)270.

[16] Q. Du, G. Gong, Nuclear Instruments and Methods in Physics Research Section A 732 (2013) 488.